Elastic scattering between two cluster nuclei ($A, B \geqslant 4$) at medium and high energies

M. M. H. El-Gogary,[1,*] A. S. Shalaby,[2] and M. Y. M. Hassan[1]
[1]*Physics Department, Faculty of Science, Cairo University, Giza, Egypt*
[2]*Physics Department, Faculty of Science, Cairo University, Beni Suef branch, Egypt*
(Received 20 April 1998)

In the framework of the Glauber multiple scattering theory, the complete expansion (which contains $2^{A\times B}-1$ terms) of the Glauber amplitude of elastic scattering between two nuclei $A, B \geqslant 4$ is obtained. Using double Gaussian density consistent with the electron-scattering experiments, the differential cross section (nuclear+Coulomb) is calculated and compared with the experimental data. It is shown that, in general, higher order terms give a substantial improvement in comparison with the previous optical limit results at relatively large scattering angles. The effect of invoking a phase-variation in the nucleon-nucleon (*NN*) amplitude is examined. We found that the presence of the phase variation improves our results, especially at the minima of the diffraction pattern. [S0556-2813(98)07012-5]

PACS number(s): 25.70.Bc, 21.30.Fe, 24.10.Cn

I. INTRODUCTION

For more than three decades, the Glauber multiple scattering theory (GMST) [1,2] has been considered as one of the most successful theories in describing hadron-nucleus elastic scattering at medium and high energies. One of the main conclusions obtained in this description is that the successive higher order multiple scattering processes, especially at large target mass number, play an important role in obtaining better fitting at high momentum transfer.

The confidence in this theory encouraged the extension of its application to nucleus-nucleus collisions, but it has been pointed out [3–6] that the analytical treatment becomes more complex and tedious in its numerical realization. This is due to the numerous multiple scattering terms ($2^{A\times B}-1$ terms) during the collision between nuclei of mass numbers *A*, *B* which make the evaluation of the scattering amplitude so difficult and lengthy. Also, the application of the conventional way of factorizing out the center-of-mass correlation [3] in the Glauber approximation leads to an unphysical divergence in the cross sections at large momentum transfer [4,6] even if we consider the full Glauber multiple scattering terms and the suitable density functions (e.g., Gaussian and harmonic oscillator functions). Although in Ref. [6] the authors showed that this divergence is removed by including the c.m. correlation to the same order as the scattering terms, but this in turn makes the numerical calculations more complicated. Owing to these difficulties, several approximation techniques have been made to simplify the calculation of the nucleus-nucleus elastic scattering amplitude [3–18]. The earlier approximation, was the so-called ''the optical limit result'' [3], and it is obtained by considering a series expansion of the optical phase-shift function in the limit of large projectile and target mass numbers. In this limit, the single scattering terms in the phase-shift expansion are only considered. The analysis of heavy-ion elastic collisions in this optical limit showed serious disagreements [4,8,14–17], especially the large *q* divergence [4]. In an attempt to remove these drawbacks, Franco and Varma [6] expanded the optical phase-shift function in terms of an infinite series, and restricted their calculations to the fourth order term in order to improve the usual optical limit (which represents the first term of this series). Also, they treated in a consistent way the c.m. correlation and the effect of the Coulomb interaction. When these calculations were applied to the 1.37 GeV α-^{12}C elastic scattering data [19], significant improvement was obtained. However, a little disagreement was observed at large scattering angles. They attributed it to the truncation of the higher order terms in the series, as well as the single Gaussian form factor employed. On the other hand, their investigations showed that the fourth order calculations are not adequate when both projectile and target nuclei become heavier. Since all the multiple scattering terms are not different, Yin *et al.* [20,21] succeeded in introducing a comprehensive method for classifying these terms into sets (referred to as orbits). Each orbit contains the scattering terms, each of which gives equal contribution to the scattering amplitude. The number of scattering terms contained in each orbit (referred to as the length of the orbit) and the orbits themselves were found with the aid of the theory of permutation groups. Using a double Gaussian density function, they applied this method to calculate the complete expansion of the scattering amplitude of ''α-α'' collision [20]. The theoretical results were in good agreement with the experimental data even at large values of momentum transfer. Further applications of the above method using various forms of Gaussian density and nucleon-nucleon (*NN*) scattering amplitude for collisions between composite systems have been carried out [22–25]. An excellent agreement of the theoretical results with the corresponding experimental data has been obtained. As a matter of fact, the method has proven to be useful for collisions between nuclei of mass numbers $\leqslant 4$. But for heavier nuclei, the expansion terms describing different multiple scattering processes became so numerous to the extent that it would be very tedious and time consuming process to classify these terms using the above-mentioned method. Recently, Huang [26] proposed an interesting technique, based on dividing the projectile and target nuclei into clusters of equal number of nucleons, in order to make the application

*Author to whom the correspondence should be addressed.

of Yin's method tractable. With elaborate treatment, Huang derived an integral formula to calculate the complete expansion of the Glauber amplitude of multiple scattering between two composite nuclei where the density function was taken to be a double Gaussian form. We calculated the elastic scattering differential cross sections for ''α-α'' collision using Huang's approach [27], and the results were in good agreement with the experimental data [28]. The success in this treatment and the absence of similar calculation for heavier masses motivated us to investigate the elastic collisions between two composite nuclei (A, $B \geqslant 4$) in the framework of the Glauber multiple scattering theory using the methods introduced in Refs. [20,26]. The full elastic scattering differential cross sections (nuclear+Coulomb) were determined by choosing a double Gaussian density function with parameters obtained by fitting the electron scattering data [29–33]. Recently, the global q-dependent phase was invoked in the NN scattering amplitude by Franco and Yin [22,23]. The authors showed that the introduction of this phase brought the Glauber model predictions closer to the experimental results for the elastic scattering of the α particle on light nuclei. Very recently, further analysis has been made [34–37] to examine whether the phase is actually important or not. This analysis, however, showed that the phase gives better account for the data of hadron-nucleus [36], α-^{12}C, and α-^{40}Ca [37] elastic scattering at high momentum transfer. Furthermore, it indicated that this phase has its strongest effect in processes where higher orders of interference are dominated. The best determination is obtained when one uses realistic nucleon density, precise nucleon-nucleon amplitudes and coupling of inelastic channels. Since the present work contains much more complicated interference of higher orders, thus it is helpful to study the role of such phase on our calculations.

The present paper contains three more sections and an appendix. Section II is devoted to the analytic expression of the nucleus-nucleus elastic scattering amplitude. In Sec. III, the results and a discussion of α-^{12}C, α-^{40}Ca, ^{12}C-^{12}C, and ^{16}O-^{12}C are presented. The conclusion is given in Sec. IV. We exhibit the orbits, the lengths, and Δ matrices (described in Sec. II) in the Appendix.

II. THEORETICAL FRAMEWORK

According to Glauber's multiple scattering theory, the elastic scattering amplitude between nuclei of mass number A, B and atomic number Z_A, Z_B may be written as [38]

$$F_{AB}(q)=H(q)\left[f^{pt}_{cZ_AZ_B}(q)+i\int_0^\infty (kb)^{2in+1} \times\{1-\exp[i\chi^E_{cz_Az_B}(\mathbf{b})+i\chi_{AB}(\mathbf{b})]\}J_0(qb)\,db\right], \tag{1}$$

where, $H(q)$ is the center-of-mass correction factor [3], q is the momentum transferred from the projectile nucleus A to the target nucleus B, k is the incident momentum of the projectile nucleus, and $\mathbf{b}$ is the impact parameter vector. $f^{pt}_{cZ_AZ_B}(q)$ is the point charge approximation of the Coulomb amplitude, $n=Z_AZ_Be^2/\hbar v$ is the usual Coulomb parameter, and $\chi^E_{cZ_AZ_B}$ is the extended charge correction to the Coulomb phase shift function. χ_{AB} is the total nuclear phase-shift function resulting from the interaction between nucleus A and nucleus B. For given projectile and target ground state wave functions, $\chi_{AB}(\mathbf{b})$ is given by

$$\exp[i\chi_{AB}(\mathbf{b})]=\langle\Psi_A(\{\mathbf{r}_i\})\Psi_B(\{\mathbf{r}'_j\})| \times\exp[i\chi_{AB}(\mathbf{b},\{\mathbf{s}_i\},\{\mathbf{s}'_j\})]|\Psi_A\Psi_B\rangle, \tag{2}$$

where $\Psi_A(\Psi_B)$ is the projectile (target) wave function, which depends on the position vectors $\{\mathbf{r}_i\}(\{\mathbf{r}'_j\})$ of the projectile (target) nucleons whose projections on the impact parameter plane are $\{\mathbf{s}_i\}(\{\mathbf{s}'_j\})$. Adopting the approximation in Ref. [6], in which χ_{AB} is equal to the sum of all NN phase-shift functions χ_{ij}, we can write

$$\chi_{AB}(\mathbf{b},\{\mathbf{s}_i\},\{\mathbf{s}'_j\})=\sum_{i=1}^{A}\sum_{j=1}^{B}\chi_{ij}(\mathbf{b}+\mathbf{s}_i-\mathbf{s}'_j). \tag{3}$$

The profile function Γ is defined in terms of the phase shift function as

$$\Gamma(\mathbf{b})=1-\exp[i\chi(\mathbf{b})]. \tag{4}$$

Hence, the total profile function takes the form

$$\Gamma_{AB}(\mathbf{b},\{\mathbf{s}_i\},\{\mathbf{s}'_j\})=1-\prod_{i=1}^{A}\prod_{j=1}^{B}[1-\Gamma_{ij}(\mathbf{b}+\mathbf{s}_i-\mathbf{s}'_j)]. \tag{5}$$

Clearly, Eq. (5) for A, $B \geqslant 4$ contains too many terms to be of any practicable use for evaluating the full multiple scattering series of the Glauber amplitude. To avoid this problem, we have used Huang's treatment [26] in which both projectile and target nuclei are assumed to have cluster structure and the classification of the scattering terms by Yin's method [20] is employed. This is performed as follows: Following Huang's method, suppose that there are M_A clusters in nucleus A and M_B clusters in nucleus B and there are M_N nucleons in each cluster (M_N should be a common divisor for the nucleus A and nucleus B), then Γ_{AB} takes the form

$$\Gamma_{AB}=1-\prod_{i=1}^{M_A}\prod_{\alpha=1}^{M_N}\left[\prod_{j=1}^{M_B}\prod_{\delta=1}^{M_N}[1-\Gamma_{i\alpha,j\delta}(\mathbf{b}+\mathbf{S}_{i\alpha}-\mathbf{S}'_{j\delta})]\right], \tag{6}$$

where $\Gamma_{i\alpha,j\delta}$ represents the profile function of scattering between the αth nucleon of the ith cluster in A and δth nucleon of the jth cluster in B. Using Yin's method in which the permutation theory is adopted to classify the scattering terms, Γ_{AB} can be reexpressed as

$$\Gamma_{AB}=-\sum_{\mu_1}^{M_1}\sum_{\lambda_{\mu_1}}T_1(\mu_1,\lambda_{\mu_1}) \times\prod_{i=1}^{M_A}\prod_{j=1}^{M_B}\left\{\sum_{\mu_2}^{M_2}\sum_{\lambda_{\mu_2}}T_2(\mu_2,\lambda_{\mu_2}) \times\prod_{\alpha=1}^{M_N}\prod_{\delta=1}^{M_N}(-\Gamma_{i\alpha,j\delta})^{\Delta_{i\alpha,j\delta}(\mu_2,\lambda_{\mu_2})}\right\}^{\Delta_{ij}(\mu_1,\lambda_{\mu_1})}, \tag{7}$$

TABLE I. Parameters of the nucleon-nucleon amplitude.

E/A (MeV/nucleon)	σ_{NN} (fm^2)	ρ_{NN}	β^2 (fm^2)	Ref.
1.08	3.35	0.45	0.07	[20]
1.27	3.95	−0.35	0.11	[20]
100	5.295	1.435	0.51	[39]
120	4.5	0.95	0.51	[39]
200	3.2	0.6	0.02	[18]
342.5	2.84	0.26	0.045	[18]

where $M_1=M_A\times M_B$, $M_2=M_N\times M_N$, $T_1(T_2)$ is the length of the orbit $(\mu_1,\lambda_{\mu_1})[(\mu_2,\lambda_{\mu_2})]$ of the permutation group $G_1=S_{M_A}\otimes S_{M_B}$ $(G_2=S_{M_N}\otimes S_{M_N})$,

$$\Delta_{ij}(\mu_1,\lambda_{\mu_1})[\Delta_{i\alpha,j\delta}(\mu_2,\lambda_{\mu_2})]$$

is the ijth ($i\alpha j\delta$th) element of the matrix

$$\Delta(\mu_1,\lambda_{\mu_1})[\Delta(\mu_2,\lambda_{\mu_2})]$$

representing the orbit. The elements of these matrices have only two values; 1 when Γ_{ij} (or $\Gamma_{i\alpha,j\delta}$) appears in the expansion term and 0 when it is absent. μ is the order of scattering and λ_μ is the serial index used to number the orbits of order μ. [All these orbits, lengths and Δ matrices are given in the Appendix.] $\Gamma_{i\alpha,j\delta}$ is related to the *NN* elastic scattering amplitude, $f_{i\alpha,j\delta}$ by

$$\Gamma_{i\alpha,j\delta}(\mathbf{b})=\frac{1}{2\pi i k_N}\int d^2\mathbf{q}e^{-(i\mathbf{q}\cdot\mathbf{b})}f_{i\alpha,j\delta}(\mathbf{q}), \tag{8}$$

where k_N is the wave number of the incident nucleon.

Assuming, for simplicity, that all the *NN* amplitudes are equal (which is approximately true at high energy), $f_{i\alpha,j\delta}$ can be parametrized by [23,37]

$$f_{i\alpha,j\delta}(\mathbf{q})=\frac{k_N\sigma}{4\pi}(i+\rho)e^{-aq^2/2}, \tag{9}$$

where σ is the *NN* total cross section and ρ is the ratio of the real to the imaginary part of the forward amplitude. a is taken to be complex; $a=\beta^2+i\gamma^2$, where β^2 is the slope parameter of the *NN* elastic scattering cross section and γ^2 is the phase variation parameter of the *NN* scattering amplitude. The parameters σ, ρ, and β^2 can all be obtained from the *NN* scattering measurements, while γ^2 is considered as a free parameter. Inserting Eq. (9) into Eq. (8), we obtain

$$\Gamma_{i\alpha,j\delta}(\mathbf{b}+\mathbf{S}_{i\alpha}-\mathbf{S}'_{j\delta})=g\ \exp[-(\mathbf{b}+\mathbf{S}_{i\alpha}-\mathbf{S}'_{j\delta})^2/2a] \tag{10}$$

and

$$g=\frac{\sigma}{4\pi a}(1-i\rho).$$

Substituting Eq. (10) into Eq. (7), Γ_{AB} takes the form

TABLE II. Best fit parameters of the nuclear density.

Nucleus	α_1^2 (fm^{-2})	α_2^2 (fm^{-2})	D	$\langle r^2\rangle^{1/2}$ (fm)
^{4}He	0.65	5	0.48	1.65
^{12}C	0.284	0.5	0.688	2.49
^{16}O	0.195	0.44	0.60	2.65
^{40}Ca	0.119	0.44	0.165	3.57

$$\begin{aligned}\Gamma_{AB}=&-\sum_{\mu_1}^{M_1}\sum_{\lambda_{\mu_1}}T_1(\mu_1,\lambda_{\mu_1})\prod_{i=1}^{M_A}\prod_{j=1}^{M_B}\Bigg\{\sum_{\mu_2}^{M_2}\sum_{\lambda_{\mu_2}}T_2(\mu_2,\lambda_{\mu_2})\\&\times(-g)^{\mu_2}\exp\Bigg[-\sum_{\alpha=1}^{M_N}\sum_{\delta=1}^{M_N}(\mathbf{b}+\mathbf{S}_{i\alpha}-\mathbf{S}'_{j\delta})^2\Delta_{i\alpha,j\delta}\\&\times(\mu_2,\lambda_{\mu_2})/2a\Bigg]\Bigg\}^{\Delta_{ij}(\mu_1,\lambda_{\mu_1})}.\end{aligned} \tag{11}$$

Now, we need to describe the wave function of the system to perform the integration of Eq. (2). Consider the approximation in which the nucleons inside any cluster and the clusters themselves inside the nucleus are completely uncorrelated. Then, we can write

$$|\Psi_A\Psi_B|^2=\prod_{i=1}^{M_A}\prod_{\alpha=1}^{M_N}\rho_A(\mathbf{r}_{i\alpha})\prod_{j=1}^{M_B}\prod_{\delta=1}^{M_N}\rho_B(\mathbf{r}'_{j\delta}), \tag{12}$$

where ρ_A and ρ_B are the normalized single particle density functions and are chosen to be of the double Gaussian type

$$\begin{aligned}\rho_r(r)=&\frac{\alpha_{1\gamma}^3\alpha_{2\gamma}^3}{(\alpha_{2\gamma}^3-D_\gamma\alpha_{1\gamma}^3)\pi^{3/2}}[\exp(-\alpha_{1\gamma}^2r^2)\\&-D_\gamma\exp(-\alpha_{2\gamma}^2r^2)]\\=&\sum_{m=0}^{1}[E'_{1\gamma}\exp(-\alpha_{1\gamma}^2r^2)]^m\\&\times[E'_{2\gamma}\exp(-\alpha_{2\gamma}^2r^2)]^{(1-m)},\end{aligned} \tag{13}$$

where

$$E'_{1\gamma}=\frac{\alpha_{1\gamma}^3\alpha_{2\gamma}^3}{(\alpha_{2\gamma}^3-D_\gamma\alpha_{1\gamma}^3)\pi^{3/2}},\quad E'_{2\gamma}=\frac{-D_\gamma\alpha_{1\gamma}^3\alpha_{2\gamma}^3}{(\alpha_{2\gamma}^3-D_\gamma\alpha_{1\gamma}^3)\pi^{3/2}}$$

with $\gamma=A,B$. α_1, α_2, and D are parameters whose values are obtained from the experimental electromagnetic form factor of the given nucleus. The incident direction of the nucleus A is chosen to be the z axis and χ_{AB} in Eq. (2) has no dependence on such variable, so the integration of Eq. (2) over z is straightforward. Thus, after integrating over z, the wave function of the system can be written as

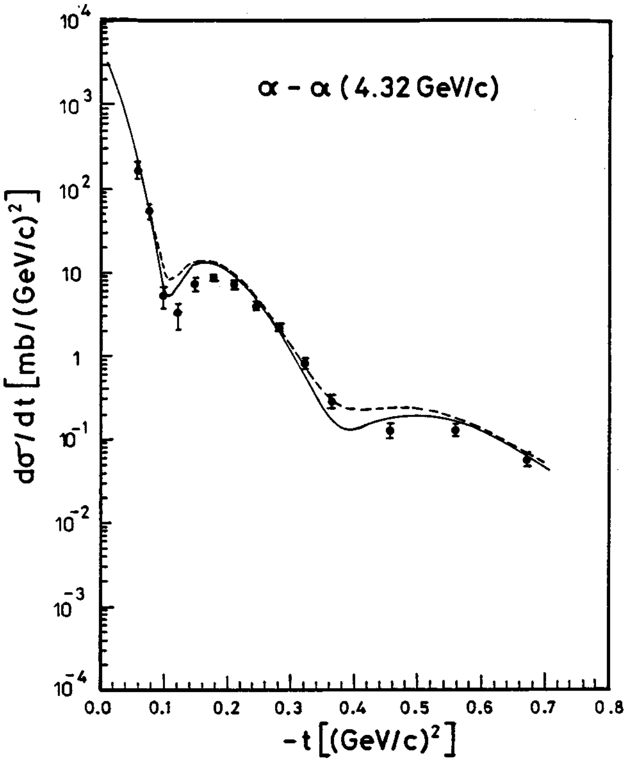

FIG. 1. Elastic differential cross section for (α-α) reaction at incident momentum 4.32 GeV/c. The dashed curve is the constant phase result ($\gamma^2=0$). The solid curve is obtained with phase variation [$\gamma^2=2\ (\mathrm{GeV}/c)^{-2}$]. The dots are the experimental data.

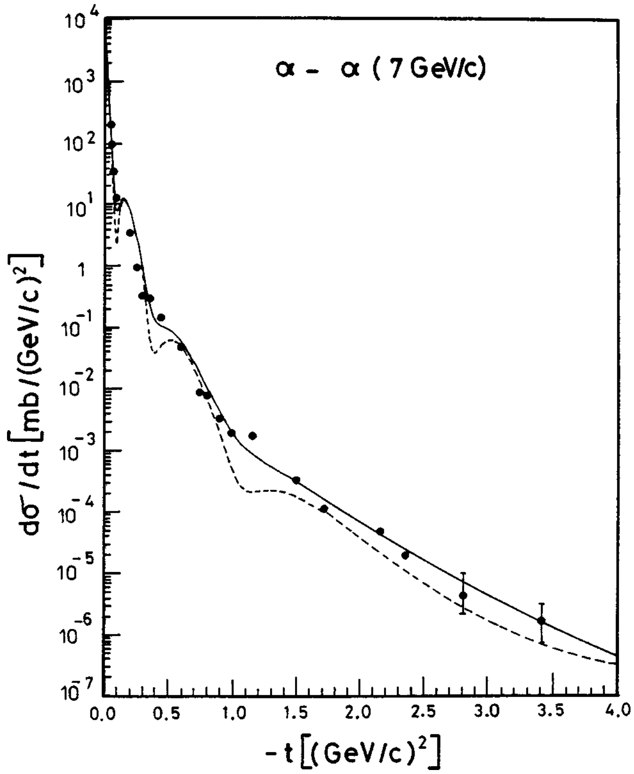

FIG. 3. Elastic differential cross section for the α-α reaction at incident momentum 7 GeV/c. The dashed curve is the constant phase result ($\gamma^2=0$). The solid curve is obtained with phase variation [$\gamma^2=5\ (\mathrm{GeV}/c)^{-2}$]. The dots are the experimental data.

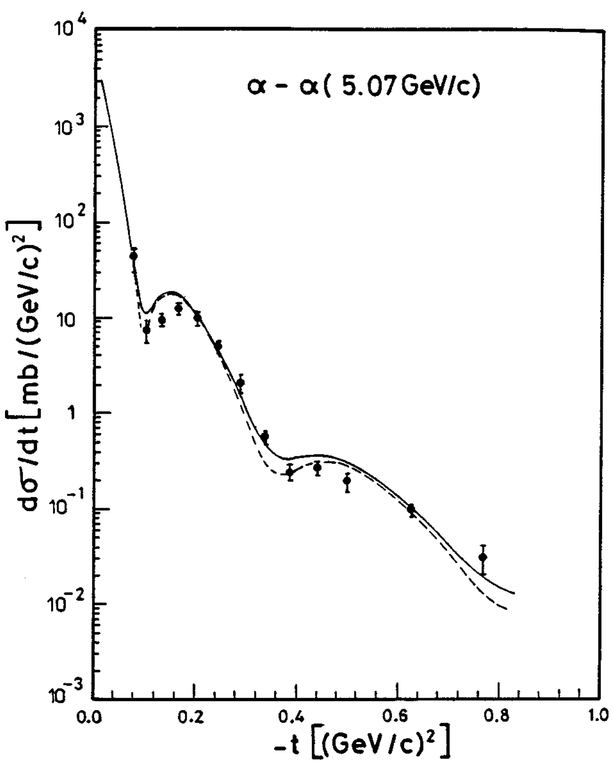

FIG. 2. Elastic differential cross section for the (α-α) reaction at incident momentum 5.07 GeV/c. The dashed curve is the constant phase result ($\gamma^2=0$). The solid curve is obtained with phase variation [$\gamma^2=3\ (\mathrm{GeV}/c)^{-2}$]. The dots are the experimental data.

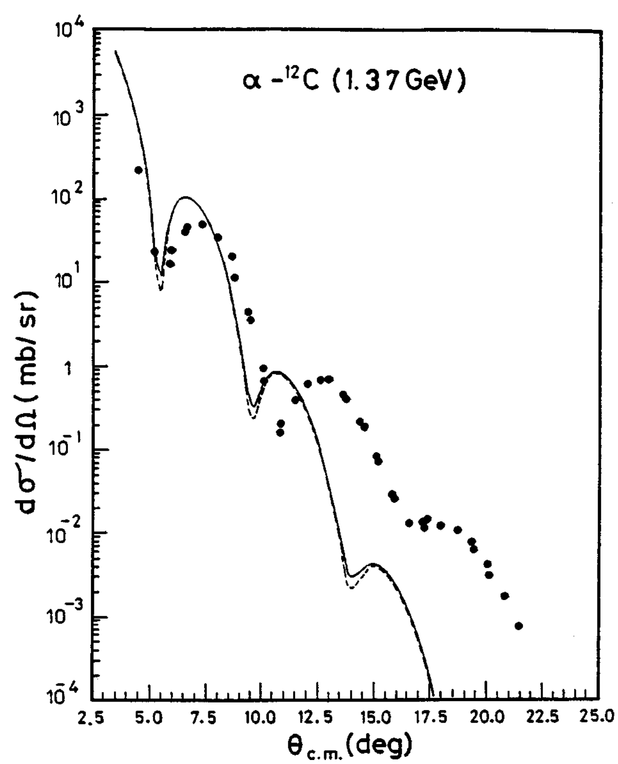

FIG. 4. Elastic differential cross section for the α-^{12}C reaction at 1.37 GeV. The dashed curve is the constant phase result ($\gamma^2=0$). The solid curve is obtained with phase variation [$\gamma^2=-2\ (\mathrm{GeV}/c)^{-2}$]. The dots are the experimental data.

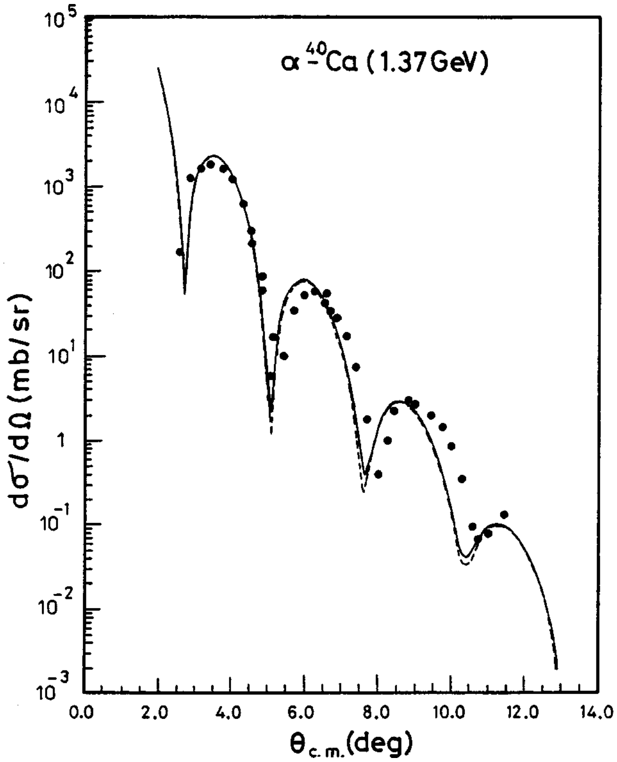

FIG. 5. Elastic differential cross section for α-^{40}Ca reaction at 1.37 GeV. The dashed curve is the constant phase result ($\gamma^2=0$). The solid curve is obtained with phase variation [$\gamma^2=-2\,(\mathrm{GeV}/c)^{-2}$]. The dots are the experimental data.

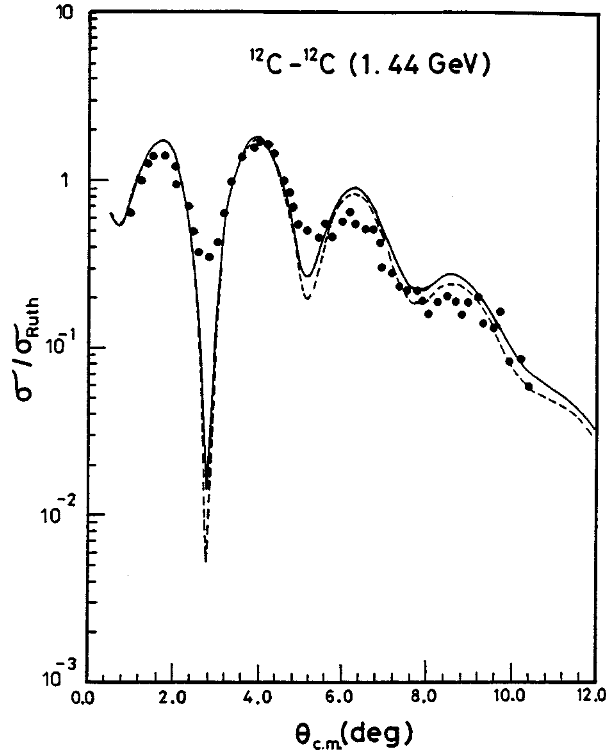

FIG. 7. Elastic differential cross section for ^{12}C-^{12}C reaction at 1.44 GeV. The dashed curve is the constant phase result ($\gamma^2=0$). The solid curve is obtained with phase variation [$\gamma^2=-3\,(\mathrm{GeV}/c)^{-2}$]. The dots are the experimental data.

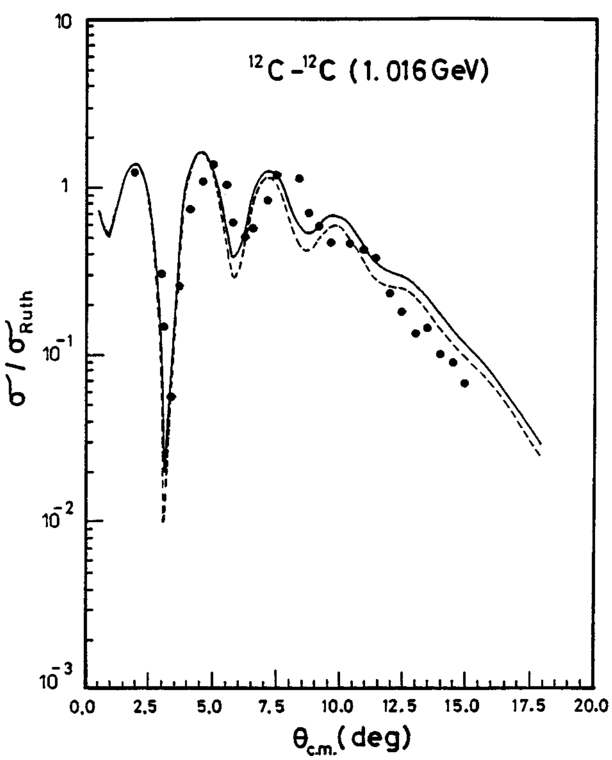

FIG. 6. Elastic differential cross section for ^{12}C-^{12}C reaction at 1.016 GeV. The dashed curve is the constant phase result ($\gamma^2=0$). The solid curve is obtained with phase variation [$\gamma^2=-3\,(\mathrm{GeV}/c)^{-2}$]. The dots are the experimental data.

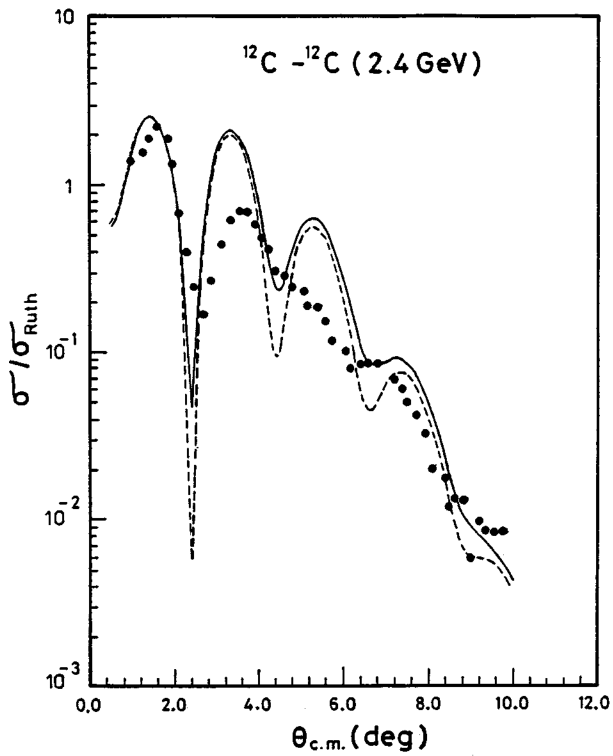

FIG. 8. Elastic differential cross section for ^{12}C-^{12}C reaction at 2.4 GeV. The dashed curve is the constant phase result ($\gamma^2=0$). The solid curve is obtained with phase variation [$\gamma^2=-8\,(\mathrm{GeV}/c)^{-2}$]. The dots are the experimental data.

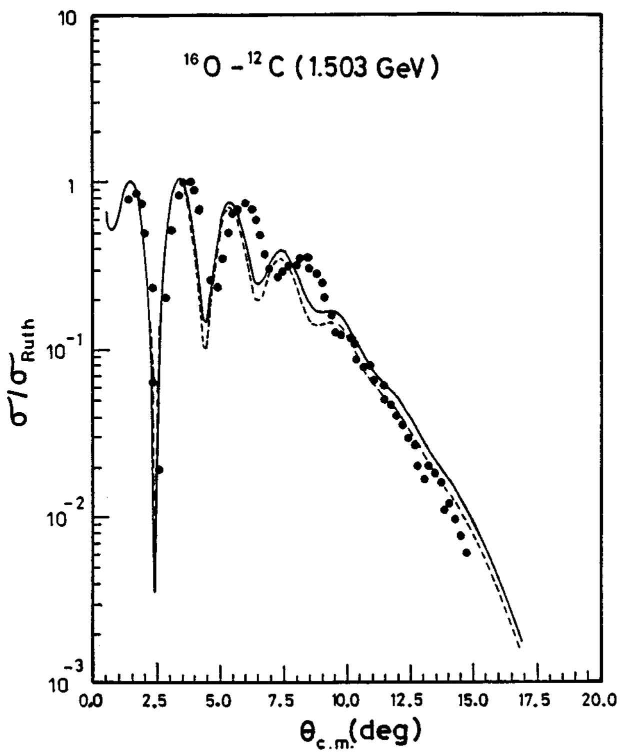

FIG. 9. Elastic different cross section for ^{16}O-^{12}C reaction at 1.503 GeV. The dashed curve is the constant phase result ($\gamma^2=0$). The solid curve is obtained with phase variation [$\gamma^2=-3\,(\mathrm{GeV}/c)^{-2}$]. The dots are the experimental data.

$$
\begin{aligned}
|\Psi_A(\{\mathbf{s}_i\})\Psi_B(\{\mathbf{s}'_j\})|^2
&=\int |\Psi_A(\{\mathbf{r}_i\})\Psi_B(\{\mathbf{r}'_j\})|^2\left(\prod_{i=1}^{M_A}\prod_{\alpha=1}^{M_N} dz_{i\alpha}\right)\\
&\times\left(\prod_{j=1}^{M_B}\prod_{\delta=1}^{M_N} dz'_{j\delta}\right)=\prod_{i=1}^{M_A}\prod_{j=1}^{M_B}\left[\left(\prod_{\alpha=1}^{M_N}\sum_{n_{i\alpha}=0}^{1}\right)\right.\\
&\times\left(\prod_{\delta=1}^{M_N}\sum_{l_{j\delta}=0}^{1}\right)C_A(n_{i1},\dots,n_{iM_N})\\
&\times C_B(l_{j1},\dots,l_{jM_N})\exp\left(-\sum_{\alpha=1}^{M_N} b_A^2(n_{i\alpha})s_{i\alpha}^2\right.\\
&\left.\left.-\sum_{\delta=1}^{M_N} b_B^2(l_{j\delta})s'^2_{j\delta}\right)\right],
\end{aligned}
$$

where

$$
\begin{aligned}
C_A(n_{i1},\dots,n_{iM_N})&=E_{A1}^{(M_N-\Sigma_{\alpha=1}^{M_N}n_{i\alpha})}\times E_{A2}^{\Sigma_{\alpha=1}^{M_N}n_{i\alpha}},\\
C_B(l_{j1},\dots,l_{jM_N})&=E_{B1}^{(M_N-\Sigma_{\delta=1}^{M_N}l_{j\delta})}\times E_{B2}^{\Sigma_{\delta=1}^{M_N}l_{j\delta}},\\
b_\gamma^2(r)&=\alpha_{1\gamma}^2(1-r)+\alpha_{2\gamma}^2\gamma,\quad \gamma=n_{i\alpha},l_{j\delta},
\end{aligned}
\tag{14}
$$

and

$$
E_{1\gamma}=\left(\frac{\sqrt{\pi}}{\alpha_{1\gamma}}\right)E'_{1\gamma},\quad E_{2\gamma}=\left(\frac{\sqrt{\pi}}{\alpha_{2\gamma}}\right)E'_{2\gamma}.
$$

TABLE III. Orbits, lengths, and Δ matrices for $G=S_2\otimes S_2$. Total number of orbits (including the orbits not shown) = 5.

μ	λ_μ	$T(\mu,\lambda_\mu)$	$\Delta(\mu,\lambda_\mu)$
1	1	4	1000
2	1	2	1100
2	2	2	1001

With the wave function (14) and the profile function (11), and after integrating over the remaining variables x and y, Eq. (2) takes the form

$$
\exp[i\chi_{AB}]=1+\sum_{\mu_1}^{M_1}\sum_{\lambda_{\mu_1}} T_1(\mu_1,\lambda_{\mu_1})\prod_{i=1}^{M_A}\prod_{j=1}^{M_B}\{Z\}^{\Delta_{ij}(\mu_1,\lambda_{\mu_1})},
\tag{15}
$$

where

$$
\begin{aligned}
Z=&\left(\prod_{\alpha=1}^{M_N}\sum_{n_{i\alpha}=0}^{1}\right)\left(\prod_{\delta=1}^{M_N}\sum_{l_{j\delta}=0}^{1}\right)\\
&\times C_A(n_{i1},\dots,n_{iM_N})C_B(l_{j1},\dots,l_{jM_N})\\
&\times\sum_{\mu_2}^{M_2}\sum_{\lambda_{\mu_2}} T_2(\mu_2,\lambda_{\mu_2})[-g]^{\mu_2}\\
&\times R[\mu_2,\lambda_{\mu_2},\Delta(\mu_2,\lambda_{\mu_2}),n_{i1},\dots,n_{iM_N},l_{j1},\dots,l_{jM_N}]\\
&\times(\exp\{-W[\mu_2,\lambda_{\mu_2},\Delta(\mu_2,\lambda_{\mu_2}),\\
&n_{i1},\dots,n_{iM_N},l_{j1},\dots,l_{jM_N}]b^2\}).
\end{aligned}
$$

The details of the integration process on x and y and the functions R and W appearing in Eq. (15) are given in Ref. [26]. Obviously, Eq. (15) in the present form has an advantage in reducing the computer CPU time spent in the calculations by restoring Z at $\Delta_{ij}=0,1$.

Finally, in order to estimate the extended charge Coulomb phase-shift function $\chi^E_{cZ_AZ_B}$, we used the same analysis as stated in Ref. [38]. The analytical formula developed using double Gaussian density functions is

TABLE IV. Orbits, lengths, and Δ matrices for $S_3\otimes S_3$. Total number of orbits (including the orbits not shown) = 25.

μ	λ_μ	$T(\mu,\lambda_\mu)$	$\Delta(\mu,\lambda_\mu)$
1	1	9	100000000
2	1	18	110000000
2	2	18	100010000
3	1	6	111000000
3	2	36	110001000
3	3	36	110100000
3	4	6	100010001
4	1	36	111100000
4	2	36	110101000
4	3	9	110110000
4	4	36	110100001
4	5	9	011100100

TABLE V. Orbits, lengths, and Δ matrices for $G=S_2\otimes S_6$. Total number of orbits (including the orbits not shown) = 49.

μ	λ_μ	$T(\mu,\lambda_\mu)$	$\Delta(\mu,\lambda_\mu)$
1	1	12	100000000000
2	1	30	110000000000
2	2	6	100000100000
2	3	30	100000010000
3	1	40	111000000000
3	2	60	110000100000
3	3	120	110000001000
4	1	30	111100000000
4	2	120	111000100000
4	3	120	111000000100
4	4	15	110000110000
4	5	120	110000101000
4	6	90	110000001100
5	1	12	111110000000
5	2	120	111100100000
5	3	60	111100000010
5	4	120	111000110000
5	5	360	111000100100
5	6	120	111000000110
6	1	2	111111000000
6	2	60	111110100000
6	3	12	111110000001
6	4	180	111100110000
6	5	240	111100100010
6	6	30	111100000011
6	7	20	111000111000
6	8	180	111000110100
6	9	180	111000100110
6	10	20	111000000111

$$\chi^E_{CZ_AZ_B}(b)=n\{M_{2A}[1+M_{2B}-M_{1B}]\times[M_{2A}E_1(\alpha^2_{1A}b^2)-M_{1A}E_1(\alpha^2_{2A}b^2)]+M_{2A}[M_{2B}E_1(C_{11}b^2)-M_{1B}E_1(C_{12}b^2)]-M_{1A}[M_{2B}E_1(C_{21}b^2)-M_{1B}E_1(C_{22}b^2)]\}, \tag{16}$$

where

$$C_{ij}=\frac{\alpha^2_{iA}\alpha^2_{jB}}{(\alpha^2_{iA}+\alpha^2_{jB})},\quad i,j=1,2,$$

$$M_{1L}=\frac{D_L\alpha^3_{1L}}{(\alpha^3_{2L}-D_L\alpha^3_{1L})}$$

and

$$M_{2L}=\frac{\alpha^3_{2L}}{(\alpha^3_{2L}-D_L\alpha^3_{1L})},\quad L=A,B$$

TABLE VI. Orbits, lengths, and Δ matrices for $S_4\otimes S_3$. Total number of orbits (including the orbits not shown) = 86.

μ	λ_μ	$T(\mu,\lambda_\mu)$	$\Delta(\mu,\lambda_\mu)$
1	1	12	100000000000
2	1	12	110000000000
2	2	18	100100000000
2	3	36	100010000000
3	1	4	111000000000
3	2	72	110100000000
3	3	36	110001000000
3	4	12	100100100000
3	5	24	100010001000
3	6	72	100100010000
4	1	36	111100000000
4	2	18	110110000000
4	3	36	110101000000
4	4	72	110100100000
4	5	72	110100010000
4	6	144	110100001000
4	7	36	011100100000
4	8	3	100100100100
4	9	24	100100100010
4	10	18	100100010010
4	11	36	100100010001
5	1	36	111110000000
5	2	36	111100100000
5	3	72	111100010000
5	4	72	110110100000
5	5	72	110101100000
5	6	36	110110001000
5	7	24	110100100100
5	8	72	110100100010
5	9	72	110100100001
5	10	72	110100010001
5	11	144	110101010000
5	12	12	011100100100
5	13	72	101100010010
6	1	6	111111000000
6	2	144	111110100000
6	3	72	111110001000
6	4	12	111100100100
6	5	72	111100100010
6	6	24	111100010001
6	7	12	110110110000
6	8	72	110110101000
6	9	24	110101011000
6	10	36	110110100100
6	11	36	110101100100
6	12	36	110110100010
6	13	144	110101100010
6	14	72	110101010001
6	15	72	110011100100
6	16	72	110110100001
6	17	18	110110001001

TABLE VII. Orbits, lengths and Δ-matrices for $S_4 \otimes S_4$. Total number of orbits (including the orbits not shown) = 191.

μ	λ_μ	$T(\mu,\lambda_\mu)$	$\Delta(\mu,\lambda_\mu)$	μ	λ_μ	$T(\mu,\lambda_\mu)$	$\Delta(\mu,\lambda_\mu)$
1	1	16	1000000000000000	7	4	288	1111100010000100
2	1	48	1100000000000000	7	5	192	1111100001000010
2	2	72	1000010000000000	7	6	288	1110111010000000
3	1	32	1110000000000000	7	7	576	1110110110000000
3	2	288	1100001000000000	7	8	96	1110111000010000
3	3	144	1100100000000000	7	9	1152	1110110010010000
3	4	96	1000010000100000	7	10	576	1110110000110000
4	1	8	1111000000000000	7	11	576	1110110000100001
4	2	288	1110100000000000	7	12	576	1110110100100000
4	3	96	1110000100000000	7	13	288	1011110011000000
4	4	288	1100101000000000	7	14	576	1011110010000100
4	5	72	1100001100000000	7	15	576	1101101001100000
4	6	288	1100001000010000	7	16	288	1101110000100010
4	7	36	1100110000000000	7	17	576	1110100100100100
4	8	576	1100100001100000	7	18	1152	0111110000101000
4	9	144	0110100010000000	7	19	16	1111100010001000
4	10	24	1000010000100001	7	20	288	1110110010100000
5	1	96	1111100000000000	7	21	1152	1110110010000001
5	2	288	1110110000000000	7	22	144	0111110010001000
5	3	288	1110100100000000	7	23	576	1110100110000100
5	4	576	1110100001000000	7	24	144	1100110000110010
5	5	576	1110100000010000	7	25	576	0110110010010010
5	6	96	0111100010000000	7	26	96	0110110010100001
5	7	576	1100101000010000	8	1	12	1111111100000000
5	8	576	1100001110000000	8	2	576	1111111010000000
5	9	144	1110100010000000	8	3	192	1111111000010000
5	10	144	1100110000100000	8	4	144	1111110011000000
5	11	576	0110110010000000	8	5	576	1111110010100000
5	12	288	1100100001100001	8	6	144	1111110000110000
5	13	144	0110100010000001	8	7	288	1111110010000100
6	1	144	1111110000000000	8	8	1152	1111110010000010
6	2	96	1111100010000000	8	9	288	1111110000100001
6	3	288	1111100001000000	8	10	288	1110110111000000
6	4	48	1110111000000000	8	11	288	1110110100110000
6	5	144	1110110100000000	8	12	288	1110111010000001
6	6	576	1110100110000000	8	13	48	1110111000010001
6	7	576	1110110000100000	8	14	288	1110111010010000
6	8	576	1110110000010000	8	15	576	1110110000110001
6	9	1152	1110010110000000	8	16	1152	1011110010100100
6	10	575	0111110010000000	8	17	576	1110100100110100
6	11	192	1110100001000010	8	18	288	1111011010001000
6	12	288	0111100001001000	8	19	1152	1101111010100000
6	13	576	1100101001010000	8	20	288	0111111010001000
6	14	144	1100110000110000	8	21	1152	1101111010000010
6	15	288	0011110010000100	8	22	288	1110110100100001
6	16	576	1110100001000001	8	23	576	1011110011000010
6	17	576	1110110010000000	8	24	144	1111110010001000
6	18	144	1110100010000001	8	25	144	1110111011000000
6	19	16	0111100010001000	8	26	144	1110110110000100
6	20	96	1100101001100000	8	27	288	1110110010100001
6	21	72	1100110000100001	8	28	576	1011011011001000
6	22	576	1100101001000001	8	29	576	1110110010010010
6	23	288	0101101001001000	8	30	288	0111101011001000
7	1	96	1111111000000000	8	31	18	1100110000110011
7	2	576	1111110010000000	8	32	72	0110110010010011
7	3	576	1111110000100000				

and $E_1(x) = -Ei(x)$ is the exponential integral function. With the results of Eqs. (15) and (16), the scattering amplitude $F_{AB}(q)$ can be obtained by performing the integration in Eq. (1) numerically. Whence the angular distribution of the elastic scattering is given by

$$\frac{d\sigma(q)}{d\Omega} = |F_{AB}(q)|^2. \tag{17}$$

III. RESULTS AND DISCUSSION

In the framework of the formalism presented in the previous section, we have calculated the elastic angular distribution for a set of nuclear reactions; namely, α-^{12}C, α-^{40}Ca, ^{12}C-^{12}C, and ^{16}O-^{12}C. The theoretical results were compared with the available experimental data given in Ref. [18]. The inputs needed to perform our calculations are the parameters included in the *NN* scattering amplitudes and the nuclear densities. For the *NN* parameters, we have used the values given in Table I. The density parameters describing the nuclei considered are determined by fitting the electromagnetic form factors measured experimentally [29–33]. Our best fit leads to the results shown in Table II.

Since the center of mass correction factor $H(\mathbf{q})$ takes a rather complicated form, we have used the approximation [37]

$$H(q) = \exp\left[\frac{q^2}{16}\left(\frac{\langle r^2\rangle_A}{A} + \frac{\langle r^2\rangle_B}{B}\right)\right],$$

where $\langle r^2\rangle_A$ and $\langle r^2\rangle_B$ are the mean square radii of the projectile and target nuclei (see Table II), respectively. We tested our codes in computing the differential cross section for α-α elastic scattering at incident momenta of 4.32, 5.07, and 7 GeV/c and the results obtained, Figs. 1, 2, and 3, agree well with the experimental data [28,40]. The results for the angular distribution of the elastic scattering of 1.37 GeV α particles on ^{12}C and ^{40}Ca nuclei are shown in Figs. 4 and 5, respectively, as dashed curves. In Fig. 4, the calculation reproduces the ^{12}C data up to the angular range $(\Theta \leqslant 9)$, while for larger angles just the qualitative trend is accounted for. Obviously, there is an overall shift for the theoretical curve toward lower angles with an underestimation for the values of the cross sections, especially at large angles. We have to mention here that although the complete expansion of the multiple scattering are considered in our calculations, no significant difference in describing the α-^{12}C data was obtained in comparison with the optical limit results presented in Ref. [18]. A more elaborate treatment of the center-of-mass correlation similar to that utilized in Ref. [6] may produce better agreement with the experimental data. For α-^{40}Ca case, Fig. 5, the theoretical situation is better than the case of ^{12}C. The data are reasonably reproduced with a smaller shift away from the forward angles. In comparison with the results for α-^{40}Ca shown in Ref. [18], our calculations gave better agreement with the experimental data in this case, especially at the minima. The predicted angular distribution of ^{12}C-^{12}C collision at the energies 1.016, 1.44, and 2.4 GeV is shown in Figs. 6–8, respectively. We observe from these figures that a substantial improvement in fitting the data is obtained, particularly at large angles, in comparison with the corresponding results given in Ref. [18]. This shows the importance of the higher multiple scattering processes. Clearly our calculation still do not reproduce successfully the experimental data at 2.4 GeV. This disagreement was attributed previously [18] to the increase in the nuclear transparency when the incident energy increases and it can be improved if one uses the coupled-channel treatment [37]. For the case of ^{16}O-^{12}C collision at bombarding energy 1.503 GeV, Fig. 9, our results are significantly better than those given in Ref. [18] especially at higher angles.

On the other hand, we have carried out an extensive numerical calculations at various nonzero values of the phase parameter γ^2 in order to investigate how the q-dependent phase $\exp[(-i\gamma^2 q^2)/2]$ invoked in the *NN* amplitude affects the nucleus-nucleus scattering. The calculations showed that for a given value of the ratio parameter ρ, the variation of γ^2 leads to either an overall increase or decrease in the estimated values of the cross sections. Indeed, we found that such a change in the cross section takes place depending on the signs of ρ and γ^2, i.e., if ρ is positive, the negative value of γ^2 increases the cross section while the positive value decreases it and vice versa. Hence, a nonzero value for ρ implies a single nonzero value for γ^2 as well. This in fact agrees with what was predicted before by Ahmad and Alvi [35] from a potential model calculation. However, the best results of the present calculations are shown by the solid curves in our figures. On comparing the solid curve (at $\gamma^2 \neq 0$) with the dashed curve (at $\gamma^2 = 0$) in each figure, we can note that the influence of the phase is obvious only at the minima and is roughly notable at the momentum transfers where no minima originally occurred. In general, taking this phase into account gives better agreement with the α-scattering data, Figs. 1–3, while the improvement is confined at the minima of the results obtained for the other reactions presented in Figs. 4–9.

IV. CONCLUSION

In the present work, the elastic scattering between two nuclei $(A,B \geqslant 4)$ has been reinvestigated by evaluating the full multiple scattering expansion of the Glauber amplitude for the collisions α-^{12}C and α-^{40}Ca at a bombarding energy equal to 1.37 GeV, ^{12}C-^{12}C at energies 1.016, 1.44, and 2.4 GeV, and ^{16}O-^{12}C at energy equals 1.503 GeV. In comparison with previous optical limit results (single scattering calculations), the calculated angular distributions obtained here showed that the inclusion of the higher order terms provides a more satisfactory fits with the experimental data, especially at large angles. As a matter of fact, the theoretical results now nicely reproduce the data of 1.37 GeV α particle on ^{40}Ca, ^{12}C-^{12}C at 1.016 and 1.44 GeV, as well as ^{16}O-^{12}C at 1.503 GeV while they are still in disagreement with the data of α-^{12}C and ^{12}C-^{12}C at 1.37 and 2.4 GeV, respectively. It is our belief that the application of the work of Franco and Varma [6] for the center of mass correlation may enhance our calculations. By invoking a phase in the *NN* amplitude, our results showed that a better agreement with the experimental data is obtained at the minima of the diffraction patterns in comparison with the free-phase calculations.

APPENDIX

This appendix contains tables in which we present the orbits, lengths, and Δ matrices employed in our calculations. We obtained them by enumerating and investigating all the possible combinations of collisions according to their permutation [20]. In the present work, the elastic collisions α-α, α-^{12}C, α-^{40}Ca, ^{12}C-^{12}C, and ^{16}O-^{12}C have been studied. Each reaction according to its assumed cluster structure needs the orbits, lengths, and Δ matrices of the groups $G_1 = S_{M_A} \otimes S_{M_B}$ and $G_2 = S_{M_N} \otimes S_{M_N}$ (defined in Sec. II). For the α-α case, we took the two-particle system as a cluster particle. Therefore, under such cluster structure $M_A = M_B = M_N = 2$. For the α-^{12}C case, the cluster structure is taken as $M_A = 2$, $M_B = 6$, and $M_N = 2$, while for the case of α-^{40}Ca, we have arranged it as $M_A = 1$, $M_B = 10$, and $M_N = 4$. For the ^{12}C-^{12}C case, $M_A = 3$, $M_B = 3$, and $M_N = 4$, while for ^{16}O-^{12}C, $M_A = 4$, $M_B = 3$, and $M_N = 4$. For the sake of brevity, we give only the tables of the nonsimilar groups (Tables III–VIII). In these tables, the first column represents the order of multiple scattering μ which ranges from 1 to $m \times n$ while λ_μ in the second column represents the serial index used to number the orbits of order μ. The third column represents the length of the orbit $T(\mu,\lambda_\mu)$. In the fourth column the $m \times n$-digit binary numbers give the Δ matrices of the group $G = S_m \otimes S_n$. The first n digits are the elements Δ_{1i}, $i = 1,2,\ldots,n$; the next n digits are $\Delta_{2i},\ldots$, and the last n digits are Δ_{mi}.

TABLE VIII. Orbits, lengths, and Δ matrices for $S_1 \otimes S_{10}$. Total number of orbits (including the orbits not shown) = 10.

μ	λ_μ	$T(\mu,\lambda_\mu)$	$\Delta(\mu,\lambda_\mu)$
1	1	10	1000000000
2	1	45	1100000000
3	1	120	1110000000
4	1	210	1111000000
5	1	252	1111100000

By symmetry, the orbits, lengths and Δ matrices for μ's, which are not shown in our tables, could be easily deduced from the tables. This is carried out by using the results for order $\mu' = m \times n - \mu$ and interchange the 0's and 1's of $\Delta(\mu',\lambda_{\mu'})$. The indices λ_μ and $\lambda_{\mu'}$ are the same and the lengths $T(\mu,\lambda_\mu)$ and $T(\mu',\lambda_{\mu'})$ are equal. The matrix $\Delta(m \times n,1)$ has elements Δ_{ij} equal 1.

[1] R. J. Glauber, *Lectures in Theoretical Physics*, edited by W. E. Brittin and L. G. Dunham (Wiley, New York, 1959), Vol. 1, p. 315.
[2] V. Franco and R. J. Glauber, Phys. Rev. **142**, 1195 (1966).
[3] W. Czyz and L. C. Maximon, Ann. Phys. (N.Y.) **52**, 59 (1969).
[4] V. Franco and A. Tekou, Phys. Rev. C **16**, 658 (1977).
[5] G. K. Varma, Nucl. Phys. **A297**, 465 (1978).
[6] V. Franco and G. K. Varma, Phys. Rev. C **18**, 349 (1978).
[7] P. J. Karol, Phys. Rev. C **11**, 1203 (1974).
[8] G. Faldt, H. Pilkuhn, and H. G. Sclaile, Ann. Phys. (N.Y.) **82**, 326 (1974).
[9] J. Hufner, K. Schafer, and B. Schurmann, Phys. Rev. C **12**, 1888 (1975).
[10] Y. Abgral *et al.*, Nucl. Phys. **A277**, 477 (1976).
[11] A. Biales, M. Bleszynski, and W. Czyz, Nucl. Phys. **B111**, 461 (1976).
[12] G. D. Alkhazov *et al.*, Nucl. Phys. **A280**, 365 (1977).
[13] J. Y. Hostachy *et al.*, Nucl. Phys. **A490**, 441 (1977).
[14] I. V. Andreev and A. V. Chernov, Sov. J. Nucl. Phys. **28**, 243 (1978).
[15] I. V. Andreev and L. A. Khein, Sov. J. Nucl. Phys. **28**, 770 (1978).
[16] R. D. Viollier and E. Turtschi, Ann. Phys. (N.Y.) **124**, 290 (1980).
[17] A. P. Gasparyan *et al.*, Sov. J. Nucl. Phys. **34**, 739 (1981).
[18] S. M. Lenzi, A. Vitturi, and F. Zardi, Phys. Rev. C **40**, 2114 (1989).
[19] A. Chaumeaux *et al.*, Nucl. Phys. **A267**, 413 (1976).
[20] Yichun Yin *et al.*, Nucl. Phys. **A440**, 685 (1985).
[21] Y. Yin *et al.*, Chin. Phys. **6**, 93 (1986); Phys. Energ. Fortis Phys. Nucl. **9**, 569 (1985).
[22] V. Franco and Y. Yin, Phys. Rev. Lett. **55**, 1059 (1985).
[23] V. Franco and Y. Yin, Phys. Rev. C **34**, 608 (1986).
[24] Zhen-qiang Tan, Zheng-Jin Lin, Pan-Ning Yan, and Chong-En Wu, J. Phys. G **16**, 1697 (1990).
[25] Zong-Jin Lin, Shu-Xia Yu, Xiang Zhong Huang, and Chong-En Wu, J. Phys. G **17**, 1159 (1991).
[26] Huang Xiang Zhong, Phys. Rev. C **51**, 2700 (1995).
[27] A. S. Shalaby, M. M. H. EL-Gogary, and M. Y. M. to Hassan, Phys. Rev. C **56**, 2889 (1997).
[28] F. L. Fabbri *et al.*, Nucl. Phys. **A338**, 421 (1980).
[29] R. F. Frosch, J. S. Mc-Carthy, R. E. Rand, and M. R. Yearian, Phys. Rev. **160**, 874 (1967).
[30] H. Grannell, Phys. Rev. **148**, 1107 (1966).
[31] J. H. Fregeaux, Phys. Rev. **104**, 225 (1956).
[32] H. F. Ehreberg, R. Hofstadter, V. Mayer-Berkhout, D. G. Rovenhall, and S. E. Sobottka, Phys. Rev. **113**, 666 (1959).
[33] N. S. Afanasiev, U. V. Kovoliov, A. S. Omelianenko, S. A. Savitzki, V. M. Khvastunov, and N. S. Shevchenko, Yad. Fiz. **5**, 318 (1967).
[34] R. J. Lombard and J. P. Moillet, Phys. Rev. C **41**, R1348 (1990).
[35] I. Ahmad and M. A. Alvi, Phys. Rev. C **48**, 3126 (1993).
[36] Ruan Wenying and Liu Youyan, J. Phys. G **21**, 537 (1995).
[37] Ji-feng Liu, Yu-shun Zhang, Chano-yun Yang, Jun-feng Shen, and B. A. Robson, Phys. Rev. C **54**, 2509 (1996).
[38] V. Franco and G. K. Varma, Phys. Rev. C **12**, 225 (1975).
[39] L. Ray, Phys. Rev. C **20**, 1857 (1979).
[40] L. Satta *et al.*, Phys. Lett. **139B**, 263 (1984).